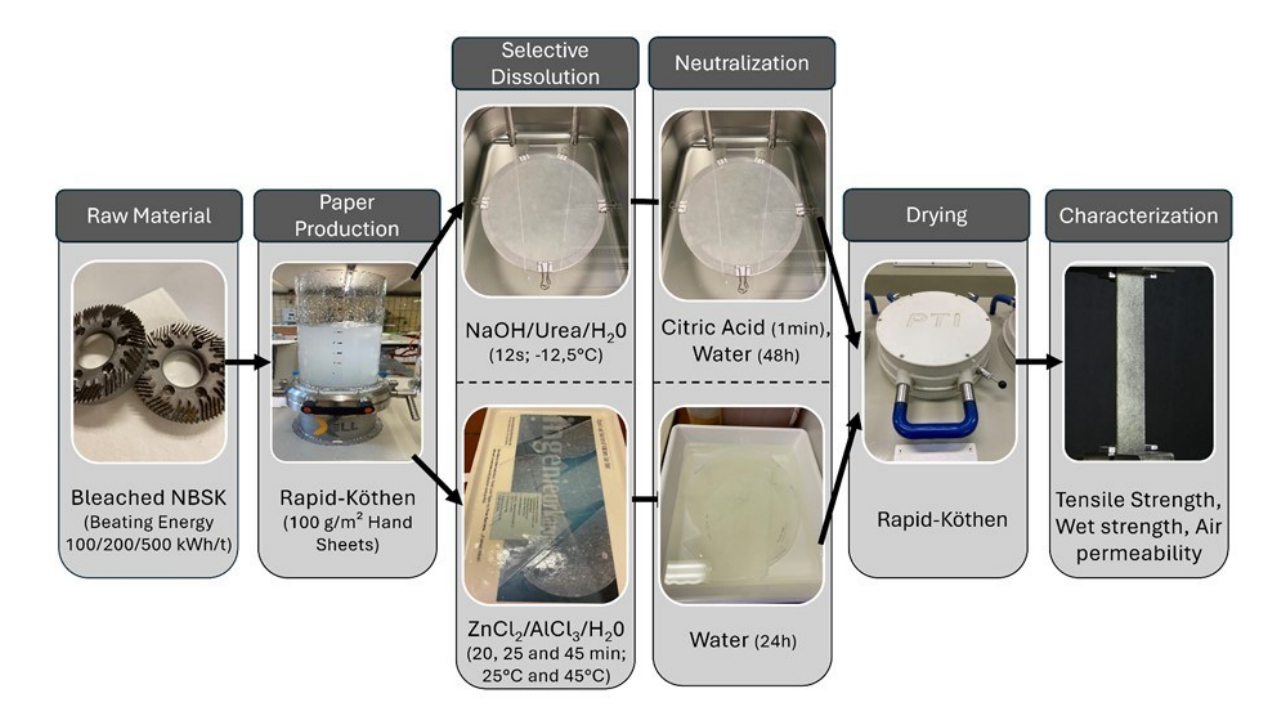
A Comparative Approach to Sustainable Paper-Based All-Cellulose Composite Production: NaOH/urea versus AlCl₃/ZnCl₂

Summer Kochersperger ,* Patrick Jahn , and Samuel Schabel

* Corresponding author: summer.kochersperger@tu-darmstadt.de

DOI: 10.15376/biores.20.3.7617-7646

GRAPHICAL ABSTRACT



A Comparative Approach to Sustainable Paper-based All-Cellulose Composite Production: NaOH/urea *versus* AlCl₃/ZnCl₂

Summer Kochersperger ,* Patrick Jahn , and Samuel Schabel

All-cellulose composites were prepared using a novel AlCl₃/ZnCl₂ molten salt solvent system, which allows for fabrication at room temperature. Unlike conventional NaOH/urea solvent systems, the proposed solvent demonstrates enhanced solubility and processing efficiency without requiring low-temperature conditions. The composites produced at room temperature, while they displayed enhanced wet strength properties, possessed a rather poor tensile strength and Young's Modulus. When the composites were treated with the molten salt solvent system at a higher temperature, the composites displayed a marked performance improvement, suggesting that the solvent's efficiency is temperature dependent. At higher temperatures comparable performance to NaOH/ urea produced all-cellulose composites was demonstrated. This dual advantage, room-temperature processing and improved properties at elevated temperatures, demonstrates the versatility of the AlCl₃/ZnCl₂ molten salt solvent system and the potential for energy-efficient, scalable production of sustainable all-cellulose composites.

DOI: 10.15376/biores.20.3.7617-7646

Keywords: All-cellulose composites; ACC; Molten salt solvent system; NaOH/urea; AlCl3/ZnCl2

Contact information: Department of Paper Technology and Mechanical Process Engineering, Technical University of Darmstadt, Alexanderstraße 8, 64283 Darmstadt, Germany;

*Corresponding author: summer.kochersperger@tu-darmstadt.de

INTRODUCTION

Increasing demand for more sustainable materials to replace plastic-based packaging has dominated the industry in the last decade. Paper fulfills a pivotal role in the packaging industry owing to the sustainability of the material, its flexibility, and its specific strength. However, paper has many functional disadvantages because it does not possess barrier properties and other characteristics that are often needed for packaging applications such as wet strength.

A potential solution to this problem is the production of all-cellulose composites (ACCs), created *via* a cellulose regeneration technique. All-cellulose composites offer numerous advantages for packaging, including high mechanical and wet strength, strong barrier properties, and sustainability due to their use of renewable materials and biodegradability (Baghaei and Skrifvars 2020). Unlike traditional natural fiber composite materials, cellulose is present in the matrix as well as in the reinforcing phase. The primary advantage of ACCs lies in improved interfacial bonding between the matrix and the reinforcing phase, due to chemical compatibility (Baghaei and Skrifvars 2020).

Two manufacturing methods are commonly used for the production of ACCs: (i) the 2-step method, which involves dissolving some cellulose in the solvent system before

manufacturing and (ii) the 1-step method involves a partial dissolution of the surface of cellulose fibers (Huber et al. 2011). The 1-step production method, widely recognized in the literature and adopted in this study, is the most common technique for ACC production.

Several solvent systems have been investigated in the literature for the production of ACCs. A good overview is given by Xi et al. (2022) in Table 1 of their work. Each of these solvent systems has limitations such as reaction temperature, reaction time, degree of polymerization (DP) of cellulose they can dissolve, and degree of solubility. The novel molten salt solvent system of AlCl₃/ZnCl₂·4H₂O shows many promising properties for a cellulose solvent, such as solubility of a wide range of celluloses up to a DP of 4080, mild reaction conditions, good stability, minor degradation of dissolved cellulose, recyclability of the molten salts used, as well as a high solubility of cellulose by weight (Xi et al. 2022). ZnCl₂ has been historically used as a cellulose solvent to create vulcanized fiber products (Letters 1932).

This novel solvent system builds off that idea, but it incorporates a small-radius aluminum ion, which improves the solubility at lower temperatures, making the solvent more efficient. It also increases the similarity to ionic liquid dissolution behavior, but at a significantly lower cost. Additionally, the salt used is recyclable, making the process more sustainable. This was confirmed by Xi et al. (2022) in their paper that introduced AlCl₃/ZnCl₂ as a suitable solvent for cellulose. Experiments have demonstrated that it is possible to recycle the inorganic salts and re-use them to dissolve the same proportion of cellulose in water up to ten times.

Even after ten recycling cycles the recovery efficiency of salt was 64% based on the initial fresh solvent. Previous literature concerning AlCl₃/ZnCl₂ in aqueous solution as a solvent for cellulose have only shown the dissolution of cellulose in the solution and have not created ACCs using this solution (Lu and Shen 2011; Shi et al. 2023; Tian et al. 2023). All of these advantageous properties make AlCl₃/ZnCl₂·4H₂O an interesting candidate for ACC production.

The study performed by Xi et al. (2022), tested the solubility of cellulose in general but did not attempt to create ACC. This work attempts to make ACCs with the AlCl₃/ZnCl₂ aqueous solvent system for the first time using a 1-step production method. Comparing lab-produced ACC results to literature is challenging due to variations in raw materials, which affect mechanical properties. To address this, this study used northern bleached softwood kraft (NBSK) pulp to enable a direct comparison of the NaOH/urea and the AlCl₃/ZnCl₂ aqueous solvent systems.

Important to note is the use of cheaper wood fiber material and not expensive high purity, chemical grade cellulose materials, as in many other publications. The primary objective is to systematically evaluate the mechanical and barrier properties of ACC produced via both solvent systems and to gain insights into the new AlCl₃/ZnCl₂ aqueous solvent system. As this work focused on paper-based ACCs, a brief investigation was done to determine if the beating of the fibers as a pretreatment also would show improvement in mechanical performance, as it does when papermaking. The refining energy was varied between 100, 200, and 500 kWh/t.

EXPERIMENTAL

Materials

Aluminum chloride hexahydrate (AlCl₃·6H₂O) \geq 95%, zinc chloride (ZnCl₂) \geq 97% and sodium hydroxide (NaOH) \geq 98% were purchased from Carl Roth GmbH + Co KG. Urea (CO(NH₂)₂) and citric acid (C₆H₈O₇) were purchased from Dr. Lohmann Diaclean GmbH in pharmaceutical quality. All chemicals were not further purified or modified before use. Mercer Stendal provided northern bleached soft kraft wood (NBSK) pulp composed of pine (40 to 70%) and spruce (30 to 60%) fiber material (see technical specifications in the Appendix).

Methods

The Voith Lab Refiner LR40 was used to beat the fibers, using a universal beating disc with the parameters 3-1.6-60. A 10-minute machine warm-up time for the beating was chosen to help reduce fiber clumps from forming. Approximately 1500 g of cellulosic material was used each time, with a moisture content of 7%. Three trials were carried out, whereby the beating energy applied were 100, 200 and 500kWh/t. Fibers with high beating energy can result in paper with higher barrier properties, due to the increased proportion of fines and the resulting increase in paper density. Increasing beating energy leads to higher fibrillation, which in turn results in increased bonding and thus improved tensile properties. When producing ACC, the dissolution of the fibers also increases fiber bonding. The solvent can penetrate the fibers best when they have been mechanically stressed. However, the densification of the papers due to increased beating may lead to a decrease in saturability, which would prevent good conversion. This is why a range of beating energies has been chosen. 500 kWh/t is not typical in industrial settings, but it is used here purely for research purposes.

For both solvent systems, reaction times were chosen to reflect times that are relevant for industrial processing. In Table 1 from Xi *et al.* (2022), the materials prepared with AlCl₃/ZnCl₂ were processed between 15 and 120 minutes based on their degree of polymerization. Bouchard *et al.* (2016) classified NBSK as having a degree of polymerization between 280 and 1910. The 120-minute processing time is associated with a degree of polymerization of 4080 in Table 1 from Xi *et al.* (2022). Trial experiments made it clear that very long reaction times provided no improvement on the material's properties. This is why longer processing times were not considered here. For the AlCl₃/ZnCl₂ solvent system, dissolution times of 20, 25, and 45 min were investigated. No optimized production procedure for ACCs using the AlCl₃/ZnCl₂ solvent system has been reported in the literature. Therefore, a higher reaction temperature was also tested to assess its impact on the mechanical and barrier properties of the final ACC samples.

Laboratory sheets with 100g/m² grammage were formed using the Rapid-Köthen sheet forming device following the EN ISO 5269-2 (2004) standard operating procedure. The sheet former used was manufactured by the company Frank PTI from Birkenau, Germany. The automatic setting was always used for the sheet formation to guarantee precise and reproducible production. Tap water with a hardness of 142.9 mg CaCO₃/L was exclusively used for all sheet forming. The drying process was also carried out using the Rapid-Köthen-Sheet forming device under standard operating conditions, applying a temperature of 93 °C for 10 min.

Laboratory ACC production using AlCl₃/ZnCl₂·4H₂O solvent

The production of ACC with the AlCl₃/ZnCl₂·4H₂O solvent system was done on a laboratory scale. Before ACC production could occur, the laboratory sheets were cut into halves so that they fit better into the laboratory trays that were used. It is important to note that sheets were conditioned for a minimum of 24 h before the cutting of the samples was performed at 23 °C and 50% relative humidity (RH) according to ISO 187 (2022). Three main steps were completed for the ACC production: dissolution, neutralization, and the drying phase. A dipping method was chosen for the dissolution phase. The solvent system was prepared according to Xi *et al.* (2022) using the following molar ratios: 0.1:0.9:4 (AlCl₃:ZnCl₂: H2O). After stirring the solvent system for 3 min at 750 rpm, the solvent was poured into a rectangular plastic laboratory tray. To reduce resource waste, a tray was chosen where the samples fit, without being too large. The tray used fit exactly half of a handsheet when laid flat. The handsheet halves were then laid into the solvent for 15 seconds, completely submerged, and laid on a large flat plastic tray for the chosen reaction time.

After the reaction time, the sheets were put into a 10 L plastic bucket filled with distilled water to neutralize. To ensure full neutralization, the neutralization was done overnight (~12 h).

The sheets were dried using the Rapid-Köthen dryer as described above and stored in a standard climate (23 °C and 50% RH) for a minimum of 24 h before characterization.

Laboratory ACC production using NaOH/urea solvent

Using the solvent system NaOH/urea, the ACC production was carried out with a custom-made automated production device *via* a dipping process. The device was designed during previous work by Jahn *et al.* (2022). The first stage of the production machine had an insulated, cooled area in which an immersion tank containing the solvent system was situated. The solvent system and the surrounding air within this chamber were cooled to a temperature of -12.5 °C. Two additional dip tanks, situated outside of the cooled area, were employed for neutralization purposes and contain a 20% citric acid solution. The transfer of the sheets between the various tanks was conducted automatically.

During the conversion process, the paper sheets were initially immersed in the solvent system for a period of 7 s. The sheet was then moved out of the solvent tank where it remained inside the cooled area for 1 s so that excess solvent dripped off. Next, the sample was transported to the neutralization tank. Leaving the cooled area, the surrounding temperature increased from -12.5 °C to room temperature.

The transport times of 4 s were added to the immersion time, resulting in a total dissolution time of 12 s. It should be noted that the ambient temperature of -12.5 °C was only ensured for the first 9 s. For neutralization, the solvent-soaked sheet was first immersed in a solution of 20% citric acid for 1 min. Thereafter, the ACC was placed in deionized water for 48 h. Finally, the ACC was dried in a Rapid Köthen sheet dryer and stored in a standard climate (23 °C and 50% RH) for a minimum of 24 h until characterization.

Characterization

Air permeability was quantified using the Gurley method (ISO 5636-5:2013) for paper and board. This method measures the time it takes for a defined volume of air to pass through a sample with a specified area.

The tensile properties of the ACC samples were determined using the ISO 1924-3 (2005) method on a Zwick Roell500 N BT1-FR0.5TN.D14 testing machine from Ulm, Germany. This test method also allows for the calculation of several parameters, as long as the thickness and grammage of the papers have been determined before testing. All mechanical testing was performed in a standard climate (ISO 187 (2022)).

Wet strength properties were determined using the DIN 54514 procedure, with samples soaked in distilled water at standard climate for 1 hour before testing.

For SEM analysis, the samples are cut to size and placed on a sample plate covered with graphite foil. To capture cross-sections, the coated papers were immersed in liquid nitrogen and then quickly cut. Otherwise, the samples are simply cut and secured to the graphite foil. For a cross-section view, sample plates with a 90° step were used, allowing a top view of the cut edge. Otherwise, flat sample plates were used. The prepared sample plates were sputter-coated with a 15 nm thick layer of platinum/palladium (80:20) using a Cressington 208 HR sputter coater. The SEM images were taken on a Zeiss EVO 10 device at an accelerating voltage of 20 kV. A secondary electron detector was used as the detector.

RESULTS

For all results presented and discussed below, the mean values of the measurements are given. The error bars indicate the standard deviation after measuring ten specimens for each sample. The results are focused on parameters that are important for packaging applications. The tensile strength gives insight into the ACC material's ability to withstand pulling or stretching forces before breaking, which are important for transport and handling of said packaging.

The Young's Modulus determines how well a packaging material will hold its shape under load and resist deformation during shipping or storage. Here, a higher Young's modulus indicates a material that is capable of resisting buckling forces. The breaking strength index allows us to better compare the tensile strength of materials as the thickness is factored out of the calculation.

The wet strength behavior describes the durability of paper packaging material and its ability to maintain structural integrity when exposed to moisture. This moisture can come from the product itself, the environment, or adverse weather conditions. Packaging materials need to be able to resist a decrease in integrity due to moisture.

Lastly, the air permeability is an indicator for packaging "breathability". A desirable air permeability depends on the product being transported. Some produce requires a breathable material for gas exchange to take place, whereas other packaged goods require a lower air permeability to protect against oxidation and moisture exposure.

Dry Tensile Properties

Figure 1 displays the average tensile strength measured for the ACC samples produced using the $AlCl_3/ZnCl_2\cdot 4H_2O$ solvent system at room temperature and 45 °C for varying beating energies and reaction times when compared to paper and NaOH/urea ACC samples.

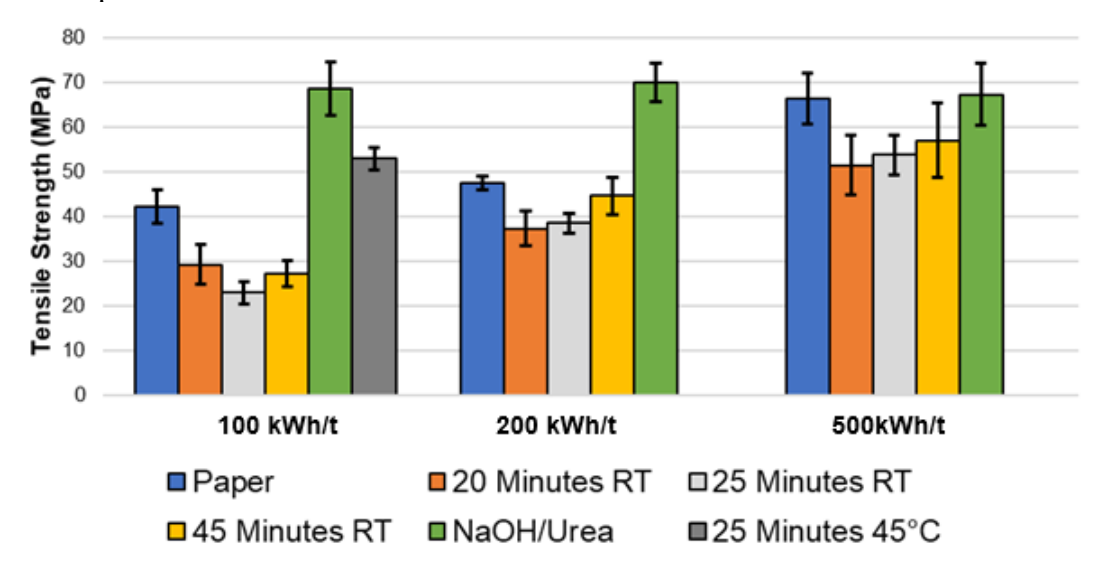


Fig. 1. Average tensile strength of ACC samples produced with the AlCl₃/ZnCl₂·4H₂O solvent system at room temperature (RT) and 45 °C, across different beating energies and reaction times. Untreated paper samples and NaOH/urea samples treated for 12 seconds are displayed for reference.

In Fig. 1, it is shown that at room temperature, the ACC samples produced using $AlCl_3/ZnCl_2\cdot 4H_2O$ performed worse than the untreated paper samples, regardless of the beating energy or the reaction time. Important to note is that at 45 °C and 25 min of reaction time, the 100 kWh/t samples displayed ~26% improvement in tensile strength when compared to the paper samples. Compared to the ACC produced using NaOH/urea, the tensile strength was approximately 15 MPa lower in value. Another important trend to note is that, with increasing beating energy, the overall tensile strength increased for the samples prepared using the $AlCl_3/ZnCl_2\cdot 4H_2O$ solvent system.

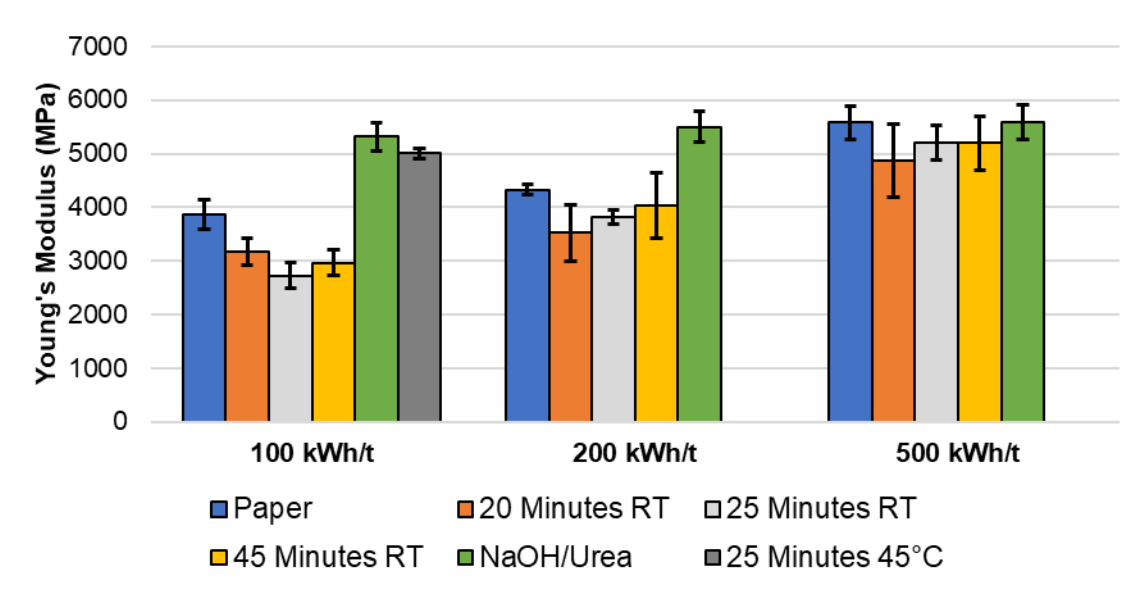


Fig. 2. Average Young's Modulus of ACC samples produced with the AlCl₃/ZnCl₂·4H₂O solvent system at room temperature (RT) and 45 °C, across different beating energies and reaction times. Untreated paper samples and NaOH/urea samples treated for 12 seconds are displayed for reference.

Despite the chemical treatment of the ACC, this improvement of the mechanical properties from beating remained. In contrast, the beating energy had little influence on the results if NaOH/urea was used as the solvent system. This is highlighted by the 500 kWh/t sample, where the untreated paper and the sample treated with NaOH/urea had very similar mean values. Upon further analysis, ANOVA tests indicate that despite similar results, they were not statistically significant (p-value= 0.801).

Figure 2 depicts the average Young's modulus for various samples of ACC produced using the AlCl₃/ZnCl₂·4H₂O solvent system as well as NaOH/urea ACC and untreated paper for reference.

The data for Young's modulus of the ACC samples produced using the AlCl₃/ZnCl₂·4H₂O solvent system showed some positive trends. An increase was observed in the material's stiffness with increasing beating energy. For the 200 and 500 kWh/t samples, a longer reaction time also led to slight increases in the stiffness of the sample. With an increased reaction temperature, an improvement of ~58.7% in the Young's modulus compared to untreated paper was measured. This was comparable to the results achieved using NaOH/urea for ACC production. Interestingly, the 100 kWh/t sample with a reaction time of 25 min at 45 °C was able to reach a similar Young's modulus as the samples with 500 kWh/t and reaction times of 25 and 45 min. Also important to note is that the increase in temperature allowed the solvent to produce a material that performed very similarly to NaOH/urea. An ANOVA analysis revealed that the results of the Young's modulus test for the NaOH/urea sample and the sample treated with AlCl₃/ZnCl₂·4H₂O at 45 °C had a high statistical significance (p-value= 0.0051). This indicates that including the variation tested across samples, there's a 0.5% probability of observing the data if the null hypothesis were true.

The dissolution and regeneration process that occurs during ACC production leads to a rearrangement and tightening of the paper fiber network, and the formation of a matrix phase, which leads to a higher Young's Modulus. As was observed at 200 and 500 kWh/t, there was an increase in the Young's Modulus over the reaction times tested. This

indicates that potentially an increase in reaction times is necessary to achieve the desired effect. The ACC production process should also form a denser, more unified fiber network with more fiber-fiber bonds. It is possible that the reaction was not fully completed before initiating the neutralization process. The influence of a higher beating energy on the Young's modulus is comparable with its influence on the tensile strength. While there was an apparent increase in the Young's modulus with increasing beating energy when using the AlCl₃/ZnCl₂·4H₂O solvent, there seemed to be no influence when using NaOH/urea.

In Fig. 3, the results for the breaking strength index are displayed. This parameter was chosen as it normalizes the breaking force over the weight of the material, thus allowing for comparison of materials and their performance regardless of thickness or weight variance. Increasing the beating energy of the fibers led to an increase in the breaking strength index for all samples. The transformation of the paper to ACC using the AlCl₃/ZnCl₂·4H₂O solvent in all cases led to a decrease in the breaking strength index when compared to untreated paper. A decrease in the breaking strength index indicates a worsening in the tensile strength of the material. Due to the breaking strength index being normalized to the grammage, an increase means that the material can achieve greater strength without an increase in weight. There was an improvement in the breaking strength index for the ACC sample by increasing the treatment temperature from 25 to 45 °C, making it comparable to 200 kWh/t ACC samples. The 200 kWh/t samples treated with the AlCl₃/ZnCl₂·4H₂O solvent system, upon further analysis ANOVA, indicated a strong statistical significance in the results with a p-value of 0.0032. This indicates that there was very little variation in the mean values measured for those samples when taking the variation into account. The ACC produced using NaOH/urea as a solvent system on the other hand showed great improvements in breaking strength compared to paper.

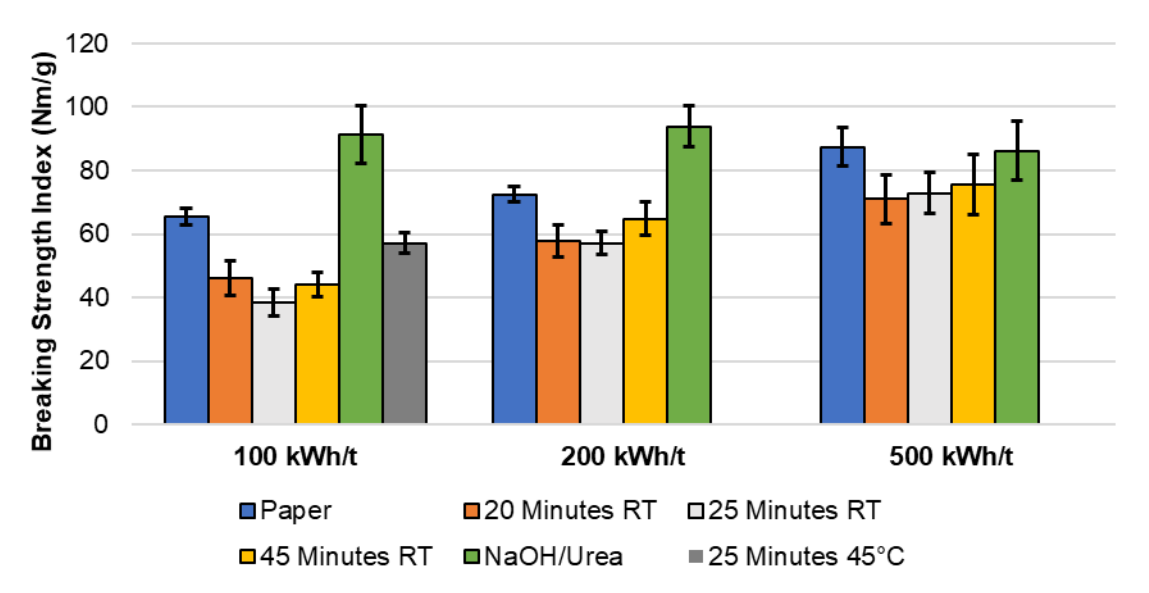


Fig. 3. Average breaking strength index of ACC samples produced with the AlCl₃/ZnCl₂·4H₂O solvent system at room temperature (RT) and 45 °C, across different beating energies and reaction times. Untreated paper samples and NaOH/urea samples treated for 12 seconds are displayed for reference.

ACC production using NaOH/urea under optimized process conditions shows the potential for increasing the breaking strength index. For the novel AlCl₃/ZnCl₂·4H₂O solvent system, significant improvements had already been achieved by adjusting the process parameters. However, there is a need for further optimization with regard to the temperature and duration of the dissolving process. With further improvement of the reaction conditions, it could be possible to achieve large breaking strength indexes without increasing fiber beating energy.

Wet Tensile Properties

Figure 4 shows that ACC was successfully created using the AlCl₃/ZnCl₂·4H₂O solvent system. This can be concluded based on the increase in wet strength properties for all specimens when compared to the untreated paper samples. An increase in wet strength behavior indicates strong fiber-fiber bonds, which in this case was facilitated by the regeneration of cellulose during the production process. Regardless of increasing beating energy, the untreated paper samples maintained the same wet strength behavior around ~1.6 ±0.1%. On the other hand, the 100 kWh ACC samples displayed the highest wet strength behavior on average compared to the other beating energies. Here, a marked improvement also was observed in wet strength behavior when the ACC production was performed at 45°C with AlCl₃/ZnCl₂·4H₂O for 100 kWh/t. An improvement of ~1082% over the value for untreated paper can be observed. No significant differences in values could be observed for the 200 kWh/t samples treated with AlCl₃/ZnCl₂·4H₂O, regardless of reaction time; this was confirmed by performing a single-variable ANOVA analysis (p-value=0.304). The same analysis was performed for the 500 kWh/t samples treated with the inorganic salt solvent (p-value=0.404).

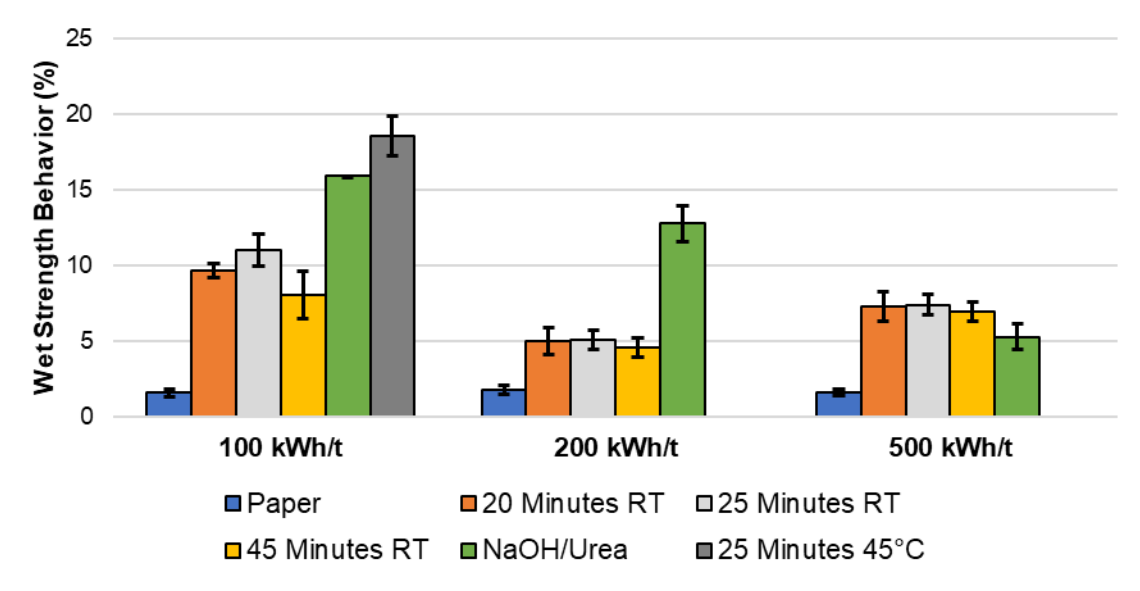


Fig. 4. Average wet strength behavior of ACC samples produced with the AlCl₃/ZnCl₂·4H₂O solvent system at room temperature (RT) and 45°C, across different beating energies and reaction times. Untreated paper samples and NaOH/urea samples treated for 12 seconds are displayed for reference.

An increase in beating energy led to a decrease in wet strength. The reason for this cannot be conclusively clarified. During production, however, it was observed that samples with higher beating energy did not become transparent. This indicates that the sheet was not completely saturated with solvent. Excessive energy can therefore reduce the permeability of the sheet to such an extent that conversion can take place only on the surface of the sheet. An examination of the wet strength of ACC produced using NaOH/urea showed great improvements compared to paper. It also confirmed that an increase in beating energy negatively impacted the wet strength. The reason for this remains unclear. The beating process may compact the base paper to such an extent that the solvent system can no longer penetrate deeply into the sheet structure, and conversion only occurs on the surface, or that fines block the pores, also preventing the solvent from penetrating the fiber network.

In Fig. 5 the Young's modulus of the wet samples is displayed. Upon treatment of the paper samples, a marked improvement in the Young's modulus was observed, despite the samples being wetted through. This is atypical for paper-based materials. Normally, water disrupts the fiber network and internal bonding by causing the fibers to swell, which leads to a reduction in the Young's modulus. An increase in the internal hydrogen bonding that occurs during the ACC production can result in a restriction of the fiber movement, which leads to an increase in the Young's modulus when the paper is wetted. Additionally, ACC materials have a higher number of crystalline cellulose domains, which retain stiffness, even in the presence of moisture, and they act as reinforcing segments along the fibers that can resist deformation. All of these phenomena can explain this increase in the Young's modulus of wet ACC materials. Here, it is apparent that an increase in the beating energy had a large impact on the average Young's modulus of the ACC samples. Interesting to also note is the increase of ~100 MPa in the Young's modulus of the ACC sample tested at 45 °C when compared to its room temperature counterparts. This is a value that exceeds even the Young's moduli of the 200 kWh/t samples. This again indicates that reaction temperature is an important parameter that needs to be explored further. For the ACC samples, which were produced using NaOH/urea, there was also a clear increase in the Young's modulus. At a beating energies of 100 and 200 kWh/t, the best Young's moduli are achieved using NaOH/urea. For samples with a beating energy of 500 kWh/t, however, the E-moduli of the ACC produced using AlCl₃/ZnCl₂·4H₂O were better. This possibly indicates that the saturation of the samples with solvent at high beating energies was even lower for the NaOH/urea solvent system compared to the AlCl₃/ZnCl₂·4H₂O solvent system.

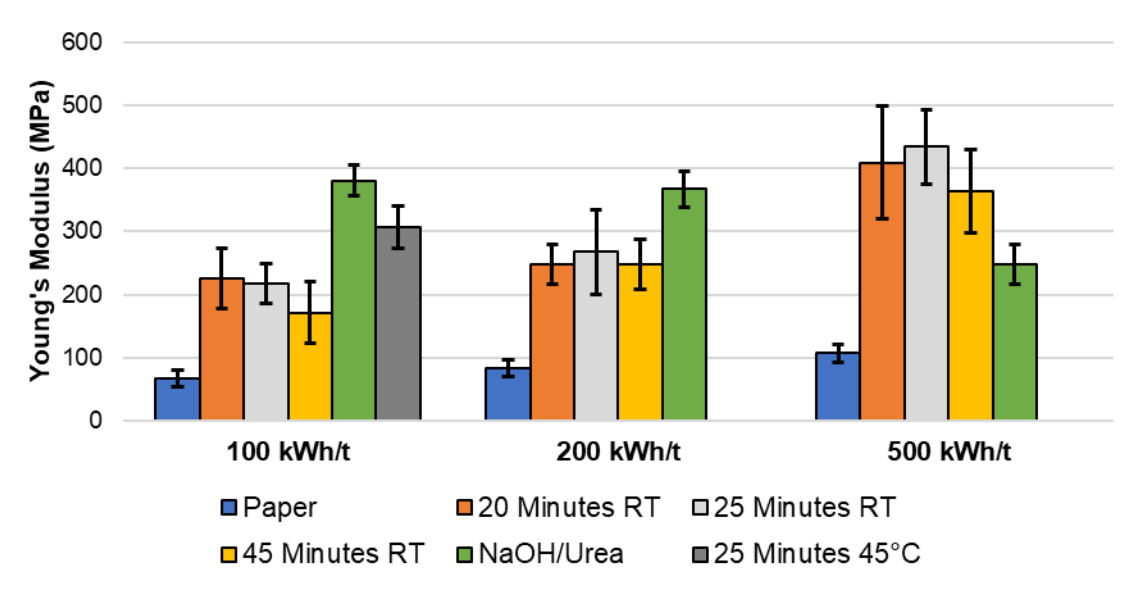


Fig. 5. Average Young's Modulus of wet ACC samples produced with the AlCl₃/ZnCl₂·4H₂O solvent system at room temperature (RT) and 45 °C, across different beating energies and reaction times. Untreated paper samples and NaOH/urea samples treated for 12 seconds are displayed for reference.

Figure 6 displays how the breaking strength index of the ACC samples tested increased when compared to untreated paper samples. This is important because a high wet breaking strength index indicates that the material can maintain its integrity and strength even when exposed to water. For ACC samples, this came from an increase in inter-fiber bonding due to the chemical treatment, which leads to matrix formation. When a material has a high wet breaking strength index, it is also less prone to swelling or structural deformation caused by water absorption. Thus, an increased wet breaking strength reflects a successful transformation of the cellulose, as hydrophobicity was increased. This is a great indication that ACC was successfully produced. An increase in the reaction temperature here showed a marked improvement in the breaking strength index of ~1296%. This result is comparable to the achieved breaking strength of ACC using NaOH/urea as a solvent system. The results of 100 kWh/t room temperature samples that were treated with AlCl₃/ZnCl₂·4H₂O indicated a statistically significant trend in the results (p-value =0.048). This indicates that the mean values were not random. This can be seen by the steady decrease in the mean values as the reaction time increases. This is a trend that is confirmed by the ANOVA test and the p-value.

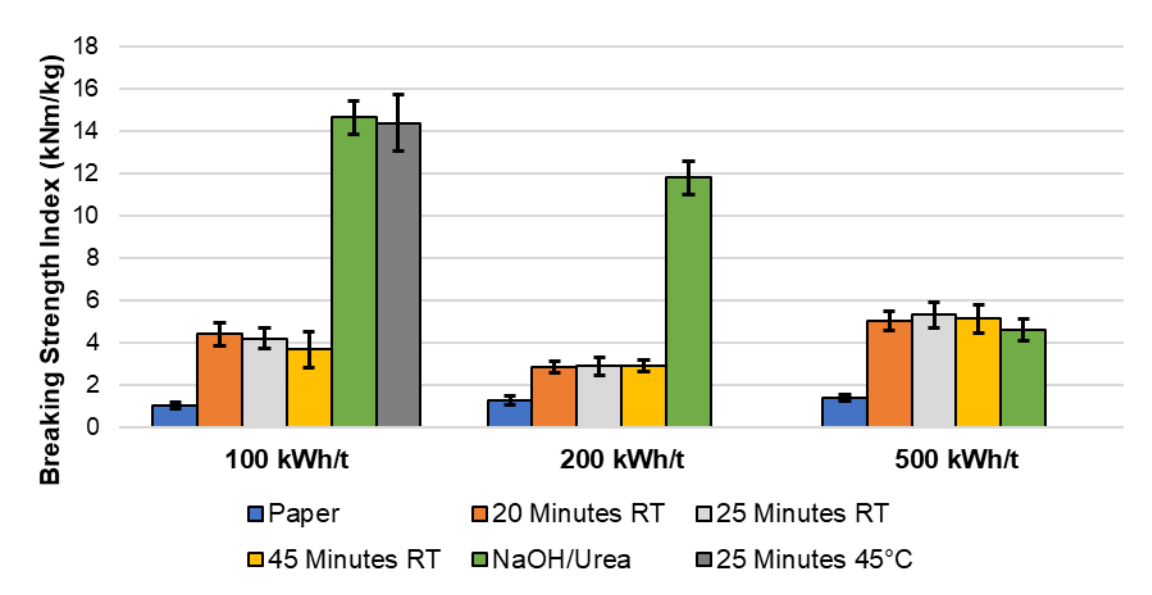


Fig. 6. Average Breaking Strength Index of wet ACC samples produced with the AlCl₃/ZnCl₂·4H₂O solvent system at room temperature (RT) and 45 °C, across different beating energies and reaction times. Untreated paper samples and NaOH/urea samples treated for 12 seconds are displayed for reference.

Air Permeability

Figure 7 shows the air permeability of the various samples tested. Due to the differences in the order of magnitude of the results, the samples are depicted on separate plots. It is important to note that the air permeability depends on the beating energy used when preparing the pulp during the paper-making process. This can be explained by the tendency to produce more fines as more beating energy is applied to the fibers. These fines then fill the pores in the paper and lead to a paper with a higher resistance to air permeation. The fibers also become more flexible, allowing them to align closer together, which increases the density of the paper. Remember that a high value here represents a lower air permeability, as in this test the time measure is how long it takes for a defined volume of air to penetrate through the fiber structure. In all three cases, it is apparent that the air permeability was negatively affected by the ACC processing using AlCl₃/ZnCl₂·4H₂O. For all AlCl₃/ZnCl₂·4H₂O samples, ANOVA tests were performed to evaluate the statistical significance of the data collected. For the 100 kWh/t samples, the ANOVA single variable analysis delivered a p-value of 0.0003, which indicates a high degree of statistical significance. This is consistent with the linearly decreasing results as the reaction time increases. Upon reaction, the papers in the solvent system for 20 min at room temperature, the data show a decrease of ~64.3%, ~56.2%, and ~41% when compared to the untreated paper's air permeability. An ANOVA analysis of the results for 200 kWh/t revealed no statistical significance in the results (p-value=0.608). The 500 kWh/t samples also resulted in a low p-value of 0.0023, due to the linearly decreasing results as the reaction time increases.

The production process should be optimized to achieve better barrier properties. The reduction of air permeability using NaOH/urea shows that improvements are possible due to the transformation from paper to ACC.

Achieving an air barrier is important for the potential application of ACCs in the packaging industry. Without an air barrier, it is not possible to achieve an adequate

oxygen barrier. This is an important step in the right direction. The oxygen barrier should be measured in future work *via* collaboration with another research institution. The reduced air permeability transforms paper from a basic wrapping material into a potentially high-performing packaging solution.

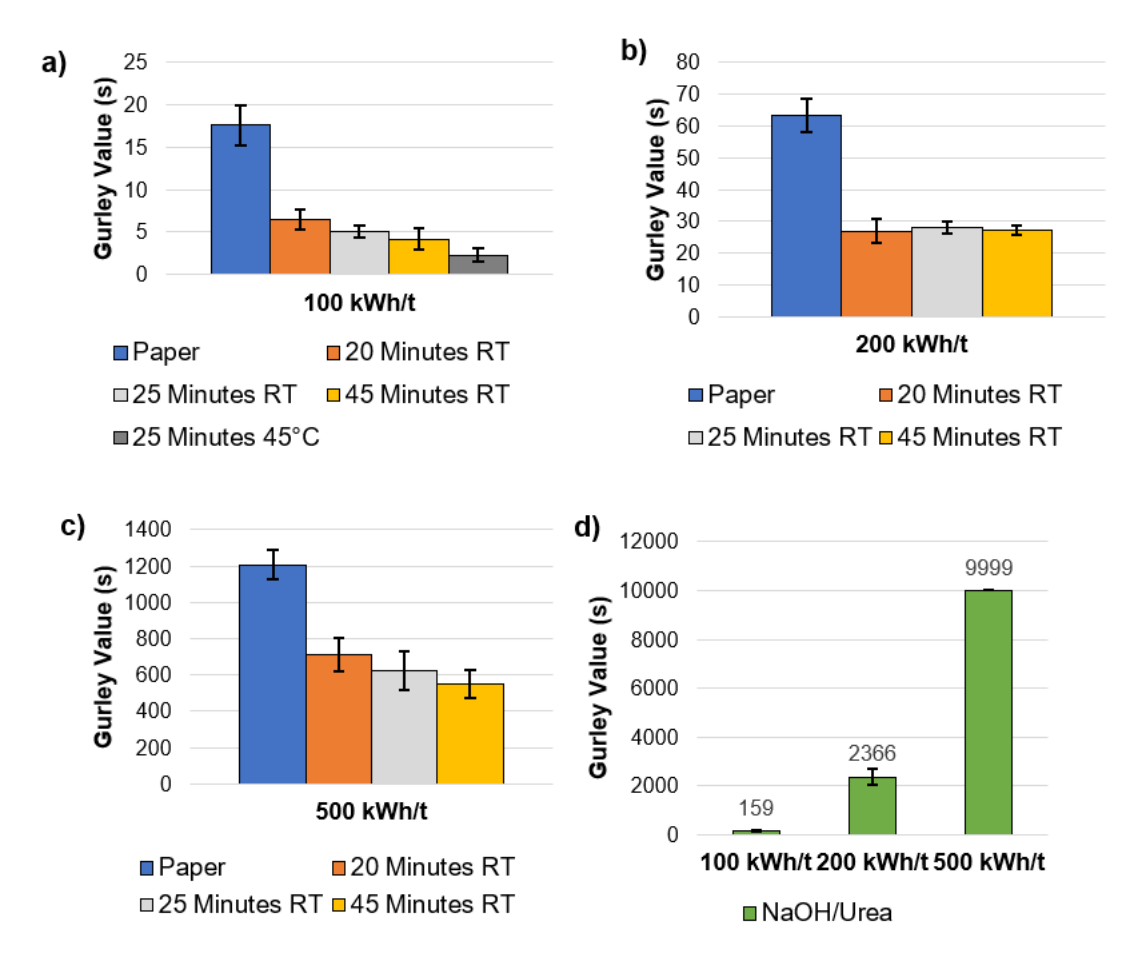


Fig. 7. Average air permeability in Gurley seconds of ACC samples prepared with AlCl₃/ZnCl₂·4H₂O with a)100kWh/t beating energy, b) with 200 kWh/t beating energy, c) with 500 kWh/t beating energy and varying reaction times at room temperature (RT) or elevated temperature. d) average air permeability in Gurley seconds of ACC prepared with NaOH/urea with varying beating energies.

Summary of Results

The purpose of this short section is to present Table 1, which summarizes the results obtained for this study.

Classification and Analysis of Results

This paper has attempted to understand key factors that influence the production of ACC with the novel molten salt AlCl₃/ZnCl₂·4H₂O solvent system. This chapter will explore some of the results in more detail and compare them not only to the NaOH/urea NBSK ACC samples produced for comparison but also to values found in the literature. In addition, unresolved aspects are highlighted that should be investigated in further research work.

Table 1. Summary of Results for ACC Samples prepared with AlCl₃/ZnCl₂·4H₂O (Solvent 1) and NaOH/urea (Solvent 2) Solvent Systems

Sample	Tensile Strength (MPa)	Young's Modulus (MPa)	Breaking Strength Index (Nm/g)	Wet Strength Behavior (%)	Young's Modulus, Wet (MPa)	Wet Breaking Strength Index (kNm/kg)	Air Permeability (s)
			100 k				
Paper	42.078	3852.835	65.529	1.572	66.661	1.030	17.632
Solvent 1, RT 20 min	29.237	3171.773	45.961	9.634	226.001	4.425	6.469
Solvent 1, RT 25 min	22.945	2727.837	38.444	11.006	217.292	4.214	5.070
Solvent 1, RT 45 min	27.127	2962.321	44.037	8.029	170.926	3.680	4.194
Solvent 1, 45°C 25 min	53.165	5010.504	57.136	18.559	306.921	14.390	2.277
Solvent 2	68.524	5317.690	91.390	15.903	380.347	14.638	159.15
			200 k	Wh/t			
Paper	47.489	4329.084	72.474	1.750	83.160	1.268	63.407
Solvent 1, RT 20 min	37.287	3520.872	57.852	4.987	248.167	2.872	27.004
Solvent 1, RT 25 min	38.458	3811.355	57.136	5.040	267.519	2.896	28.173
Solvent 1, RT 45 min	44.677	4027.310	64.777	4.550	248.348	2.905	27.343
Solvent 2	70.050	5501.733	93.922	12.754	366.940	11.812	2365.84
			500 k	Wh/t			
Paper	66.467	5581.359	87.378	1.611	107.066	1.408	1207.113
Solvent 1, RT 20 min	51.455	4868.715	70.935	7.244	409.372	5.048	714.29
Solvent 1, RT 25 min	53.757	5195.034	72.927	7.389	434.816	5.325	626.474
Solvent 1, RT 45 min	56.995	5200.241	75.689	6.939	364.540	5.128	551.274
Solvent 2	67.309	5580.390	86.102	5.268	248.077	4.587	9999

Material properties

Tensile test results from the literature for various pulps can be seen in Table 1. Based on data shown in the table, the results for the $AlCl_3/ZnCl_2 \cdot 4H_2O$ solvent system at 45 °C and NaOH/urea using 100 kWh/t bleached NBSK as starting material are added for comparison. In Table 1, tensile strength (S), Tensile Index (TI), Elastic Modulus (E^*), and Grammage (G) are presented.

The results in Table 1 from Tervahartiala *et al.* (2018) indicate that the treatment of paper made from different fibers with chemicals to transform them into ACC had differing effects. Softwood pulps appear to show a marked improvement in properties. Samples from hardwood *i.e.* eucalyptus showed an improvement in properties as well, whereas non-wood fiber materials such as abaca where treatment negatively impacts the tensile properties (Tervahartiala *et al.* 2018). It must be mentioned that the tensile properties of paper are heavily dependent on grammage, which as Table 1 highlights, varied across samples.

Table 2. Tensile Strength of ACC Samples (UT/untreated, T/treated) *vs.* AlCl₃/ZnCl₂·4H₂O ACC Bleached NBSK at 45 °C and NaOH/urea Bleached NBSK at -12.5 °C (Tervahartiala *et al.* 2018)

Pulp	UT/T	S (N/m)	TI (Nm/g)	<i>E</i> *(GPa)	G (g/m ²)
Bleached Pine	UT	1332	16.5	1.7	80.6 ± 2.0
Bleached Pine	Т	5735	61.0	4.7	94.1 ± 1.8
Unbleached Pine	UT	1478	18.3	1.9	80.6 ± 1.3
Unbleached Pine	Т	5474	53.6	3.5	102.2 ± 3.1
Bleached Spruce	UT	32	12.8	1.4	79.6 ± 1.1
Bleached Spruce	Т	530	51.0	3.8	95.3 ± 2.4
Bleached Eucalyptus	UT	59	17.8	2.1	78.6 ± 1.2
Bleached Eucalyptus	Т	246	35.5	3.0	86.3 ± 5.8
Bleached Abaca	UT	338	44.8	3.2	80.6 ± 1.4
Bleached Abaca	Т	93	34.5	2.0	113.8 ± 4.1
Bleached NBSK	UT	6471	65.02	3.2	97 ± 10.7
Bleached NBSK	T with AICl ₃ /ZnCl ₂ ·4H ₂ O	7943	82.1	5.0	99 ± 10.6
Bleached NBSK	T with NaOH/urea	9195	91.4	5.3	100.7 ± 2.1

At the bottom of the table, the values for untreated NBSK and treated NBSK have been added. For the NBSK treated with AlCl₃/ZnCl₂·4H₂O, the values displayed are those of the sample produced using a solvent system temperature of 45 °C. When considering the percentage increase for each property, between the treated and untreated samples, some interesting trends can be seen.

The treatment of abaca, a type of non-wood fiber, led to a decrease in all properties displayed in Table 2. Both NBSK samples had percentage increases in the tensile strength between abaca at -72.5% and unbleached pine at 270%. NBSK treated with AlCl₃/ZnCl₂·4H₂O showed an improvement of 22.8% in tensile strength upon treatment and NBSK treated with NaOH/urea showed an increase of 42.1%. Tensile index values for both treated NBSK samples lay above the abaca fibers and below the bleached eucalyptus fibers. The elastic modulus change after treatment showed a different trend. Here, both samples of treated NBSK showed improvements in the elastic modulus above eucalyptus at 42.9% and below unbleached pine at 84.2%. The NBSK treated with NaOH/urea showed an improvement in the elastic modulus of 65.6% and the sample treated with AlCl₃/ZnCl₂·4H₂O showed an improvement of 56.3%. With improvement of the ACC production parameters for AlCl₃/ZnCl₂·4H₂O, achieving even better results is attainable, as preliminarily demonstrated in this study; however, further research is required. Higher reaction temperatures would be expected to increase the speed of the reaction and the penetration of the solvent, which seems to be the

dominating factor to creating better ACC materials. These parameters need to be optimized.

Further literature results, displayed in Table 3 below, provide more insight into further mechanical and barrier properties measured for ACC samples.

Table 3. Mechanical and Barrier Properties of ACC Samples as Reported by Literature with Varying Solvent Systems in Comparison with the Results from this Study (Ma *et al.* 2014; Yousefi *et al.* 2015; Jiao *et al.* 2015; Tanaka *et al.* 2018; Guzman-Puyol *et al.* 2019; Ma *et al.* 2015; Yousefi *et al.* 2011)

Cellulose Raw Material	Solvent System	Tensile Strength	Young's Modulus	Wet Strength	Air Permeability	Other Barrier Properties Tested
Filter Papier	NaOH/urea	80 Nm/g	-	20.73 Nm/g (33.8 %)	-	Grease resistance
Canola Straw	LiCL/DMA	210 MPa	19.7 GPa	ı	0 µm Pa−1 s−1	-
Filter paper	NaOH/urea/Zn O	211 MPa	-	ı	1	Grease resistance
Bleached pine kraft pulp	1-ethyl-3- methylimida- zolium acetate	65 Nm/g	3.2 GPa	18.23 Nm/g (> 20 %)	0.265 ml/min	
Cellulose nanofibers	trifluoroacetic acid:trifluoroace tic anhydride	84 MPa	4.78 GPa	-	-	Water vapor Permeability
Filter paper	ZnO	8-9 kN/m*	-	1	-	Grease resistance
Canola Straw	1-Butyl-3- methylimidazoli umchlorid	208 MPa	20 GPa	no	0 µm Pa−1 s−1	-
NBSK	AlCl ₃ /ZnCl ₂ ·4H ₂ O, 45°C, 100kWh/t	53.165 MPa	5.01 GPa	18.56%	2.28s	-
NBSK	NaOH/urea, 100 kWh/t	68.52 MPa 81 Nm/g	5.32 GPa	15.90%	159.15 s	-

The cited authors used a variety of raw materials as well as a variety of solvent systems to produce ACC samples. A direct comparison of the results is difficult due to the diverse production parameters. Nevertheless, the results show the range of material properties. Unfortunately, not every study contains all the parameters that were measured in the present work; however, a variety of cellulose raw materials and solvent systems are covered in the table for the best possible comparison. The values from literature were converted to similar units used in this paper for better comparison when possible.

The mechanical properties under tensile load are comparable with ACC from the studies of Ma *et al.* (2014) and Tanaka *et al.* (2018), which were produced from paper and wood pulp. The use of annual plants such as canola straw often enables the production of ACC with higher tensile strength. This finding is supported by Yousefi *et al.* (2011). The high tensile strengths achieved in the study by Jiao *et al.* (2015) using filter paper as a raw material are surprising.

As a result of the conversion process, improvements in wet strength were achieved using both solvent systems. The best wet strength properties obtained were slightly smaller compared to the results from other publications. Tanaka *et al.* (2018) produced ACC from paper with ionic liquids as a solvent system, resulting in a wet strength of 18.2 Nm/g. In a study investigating the effect of NaOH/urea solution on the properties of paper from Ma *et al.* (2014) wet strength properties of up to 20.7 Nm/g were achieved, or 33.8%.

Using the solvent system AlCl₃/ZnCl₂·4H₂O, a conversion from paper to ACC led to an increase in air permeability. In another publication, it is shown that an excellent improvement in barrier properties can be achieved by converting paper to ACC. Tanaka et al. (2018) have shown that the treatment of conventional paper made from bleached pine kraft pulp with an ionic liquid affects air and oxygen permeability. The air permeability of the starting material could be reduced from 3880 mL/min to 0.265 mL/min for ACC at optimal process conditions. In another study by Yousefi et al. (2015) it was shown that ACC can be produced using the DMAc/LiCl solvent system and that the product was almost impermeable to air. The experiments using NaOH/urea conducted as part of this study led to major reductions in air permeability. Compared to the values obtained in literature, the barrier effect achieved was nevertheless low. Based on the investigations carried out, the exact causes of this cannot be fully determined. Considering the relevant barrier properties for the packaging industry, further research into this is desirable.

As previously mentioned, the diverse parameters that influence the ACC properties make it difficult to compare different studies in the field of ACC research. In order to gain a deeper understanding of the interactions between influencing parameters during production and the resulting material properties, it would therefore be advisable to carry out further studies. In said studies only individual parameters should be varied and the results should be compared to literature in detail.

Material Changes – SEM Observations

To further understand the trends observed in the data, specifically the decrease in wet strength with increased beating energy, a closer examination of the ACC material's structure was conducted using an SEM Microscope. The working hypothesis is that due to the increased beating energy, which inherently produces more fines, the pores of the paper matrix become inaccessible to the solvent, leading to less conversion of the inner paper structure. It is suggested that a true sandwich structure is formed, and when samples are cut into strips for the wet strength test and laid in water, the water can easily penetrate the middle of the paper matrix, thus weakening the paper structure more than if the conversion in the thickness direction were more successful. To support this hypothesis, SEM pictures were taken of the surface and cross-section for every sample type. To facilitate a focused discussion, only untreated lab sheets and ACC samples from each solvent system with the best dry mechanical properties were chosen to be analyzed in this section.

First, the surface SEM pictures of the ACC material will be presented in comparison with the untreated lab sheet. Figure 8a-c displays the different samples of 100kWh/t paper samples, either untreated (Fig. 8a) or treated. Figure 8a) exhibits a highly porous surface with large, irregular pores. The fibers have a coarse appearance and show minimal flattening or fusing. All of these observations indicate a minimal presence of regenerated cellulose, which is consistent with the fact that Fig. 8a, is the untreated lab

sheet. Figure 8b displays a surface that is relatively dense in appearance. The fibers are tightly woven, but there appear to be more pores. The surface also shows signs of partial dissolution in some areas where the fibers are fused together. Figure 8c has a more irregular structure with large open pores. It is possible that the chemical treatment led to uneven regeneration. The fiber edges appear more defined here, which indicates less cellulose regeneration.

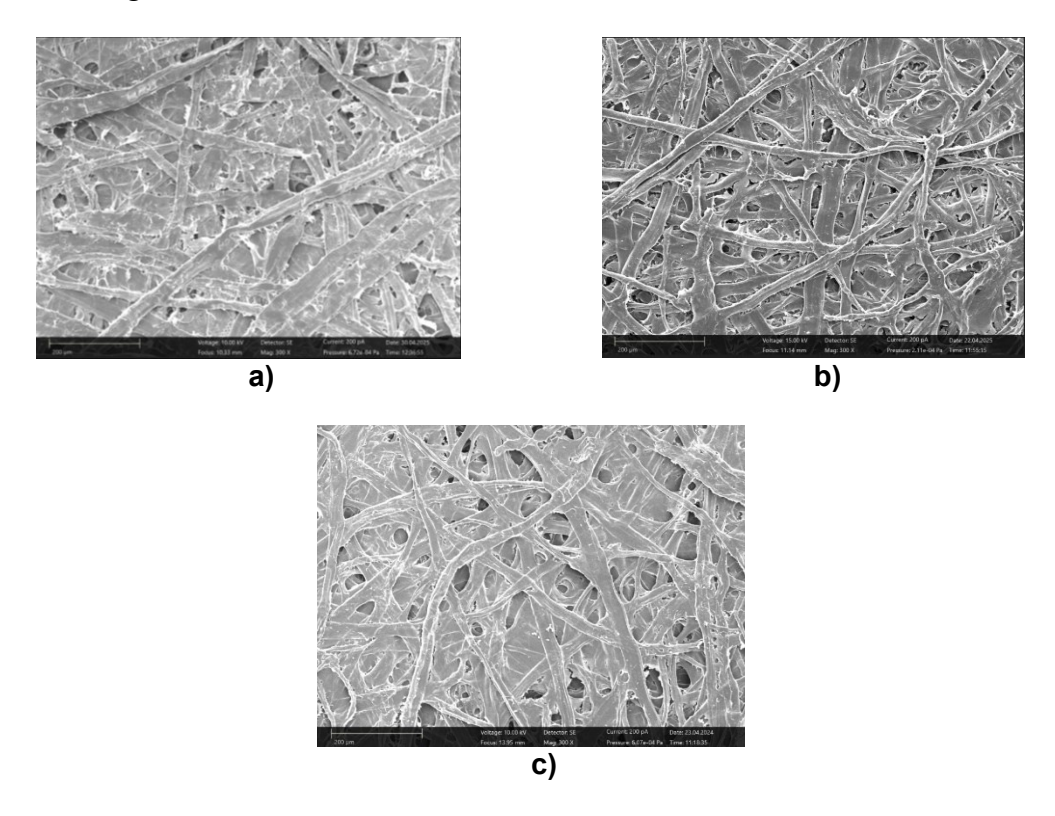


Fig. 8. SEM pictures of 100kWh/t samples. a) 100 kWh/t lab sheet, 300x magnification, b) 100 kWh/t AlCl3/ZnCl2 25 Min at 45°C, 300x magnification, and c) 100 kWh/t NaOH, 300x magnification

In order to enable a quantitative comparison of the porosity between samples, image analysis tests were carried out. The images in Fig. 8 were converted to binary (black/white) images to identify the porosity of the materials using ImageJ (see Appendix). Image J was used to analyze the percentage of the area identified as pores (black) *versus* solid fiber regions (white) using adaptive thresholding to account for local brightness variations. As one can see from the binary images included in the Appendix, this method is not suitable for identifying the porosity of the material. The clear separation of fibers and pores was not achieved. This is most likely due to the nature of the material being 100% cellulose; thus, the density and appearance of the fibers as well as the matrix, appear very similar in the SEM images. The image analysis software is unable to successfully distinguish between the fibers and the pores of the ACC material. Further quantitative methods were not explored to evaluate the images.

Inspecting the images of the 200kWh/t samples, as pictured in Fig. 9, can provide insight into the effectiveness of the chemical treatment to transform the materials into ACC. Figure 9a displays a very porous fiber network with many voids and visible, distinct fiber boundaries, which is to be expected from an untreated sample.

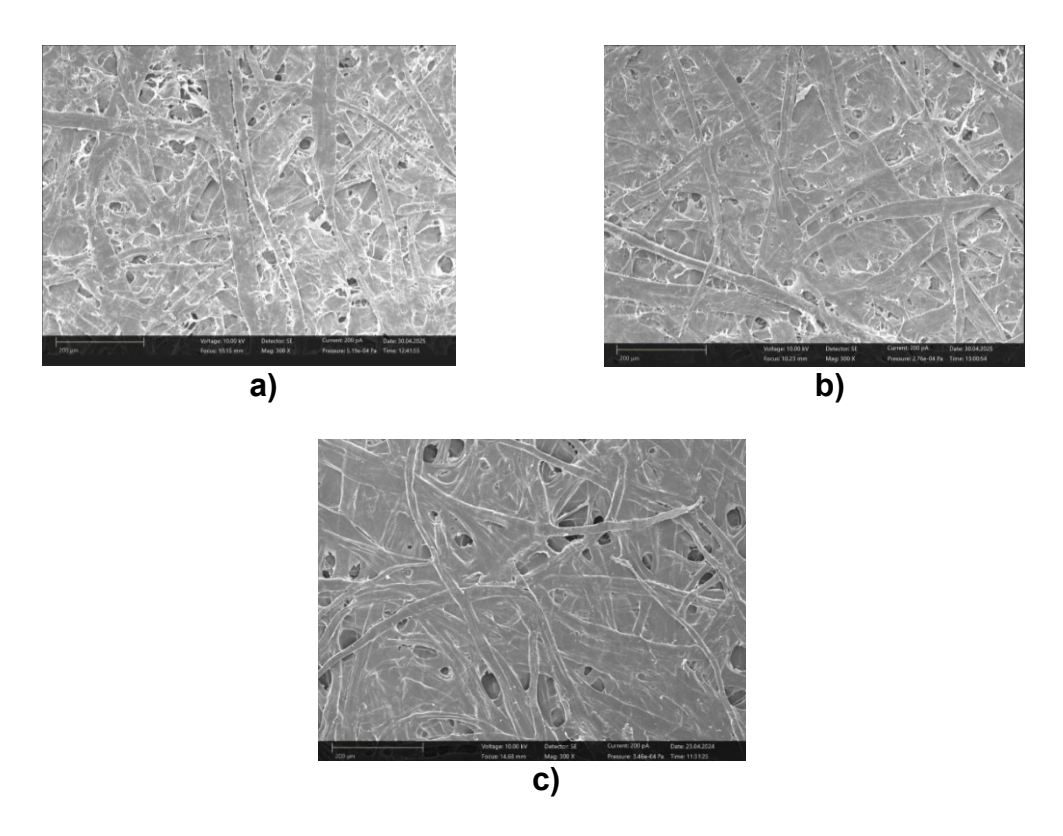


Fig. 9. SEM pictures of 200kWh/t samples. a) 200 kWh/t lab sheet, 300x magnification, b) 200 kWh/t AlCl3/ZnCl2 45Min, 300x magnification, and c) 200 kWh/t NaOH, 300x magnification

Figure 9b, with a 45-minute treatment in the AlCl₃/ZnCl₂ solution, shows a mostly smooth material surface with some smaller pores throughout. The fibers appear to be only partially bonded and are homogeneous in texture. This indicates a sample with a mildly effective ACC treatment. Figure 9c contains an SEM image of the 200 kWh/t sample treated with NaOH/urea. The sample appears to have the smoothest and least porous surface. Many fibers have fused or lost their boundaries, indicating a high level of regeneration. The denser surface indicates that regenerated cellulose is forming a continuous matrix along the material surface. This sample displays the highest degree of fiber to matrix conversion and a well-formed surface.

Upon observing the 500 kWh/t samples in Fig. 10, it can be seen that the samples were generally compact and denser in structure than previously observed samples. This is most likely due to the increased mechanical treatment and subsequent chemical conversion. Figure 10b exhibits a compacter fiber structure than the untreated sample in a). Figure 10b has pores that are smaller and fewer in number than previous samples, which suggests high consolidation of the material surface. This sample appears to have been treated more than the others. Figure 10c exhibits a largely smooth and dense material surface, with an almost plastic-like appearance. There were minimal open pores, and the majority of fibers had lost their original structure. Fewer fiber edges are visible when compared to other samples. These are strong indications that cellulose regeneration had taken place.

Cross-section SEM images

It must be noted that the samples treated with NaOH/urea, as well as some of the lab sheet samples were prepared using a razor blade/scapel and the other samples were cut using microscopy scissors.

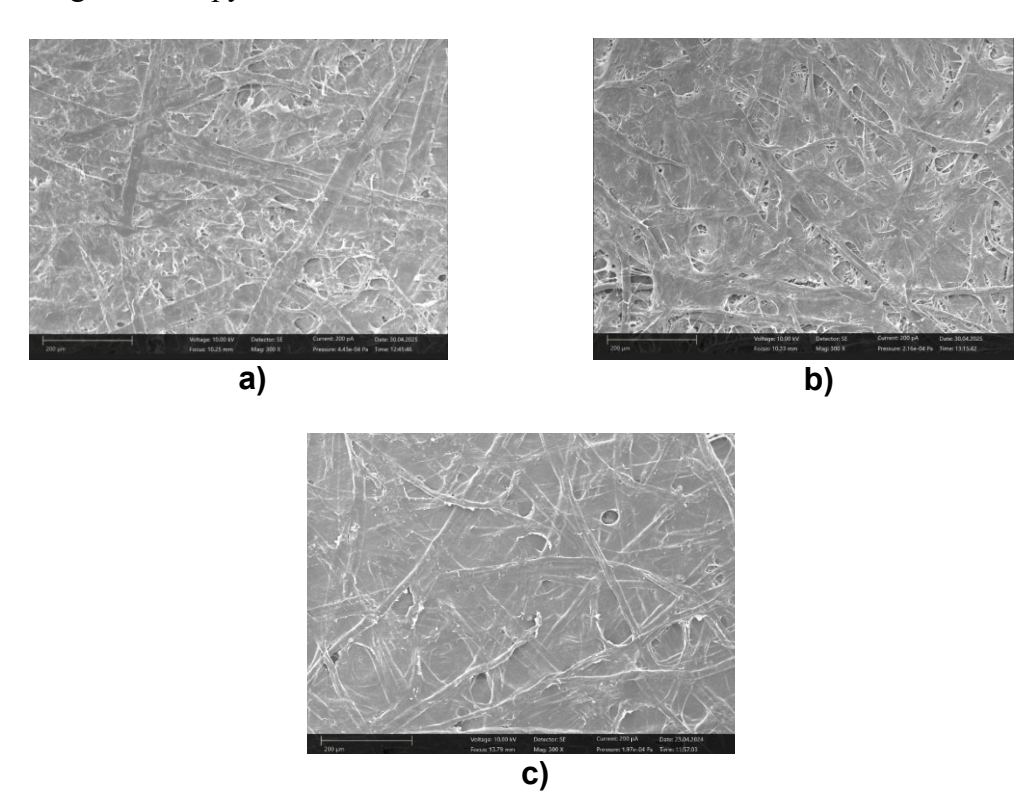


Fig. 10. SEM pictures of 500kWh/t samples. a) 500 kWh/t lab sheet, 300x magnification, b) 500 kWh/t AlCl3/ZnCl2 45Min, 300x magnification, and c) 500 kWh/t NaOH, 300x magnification

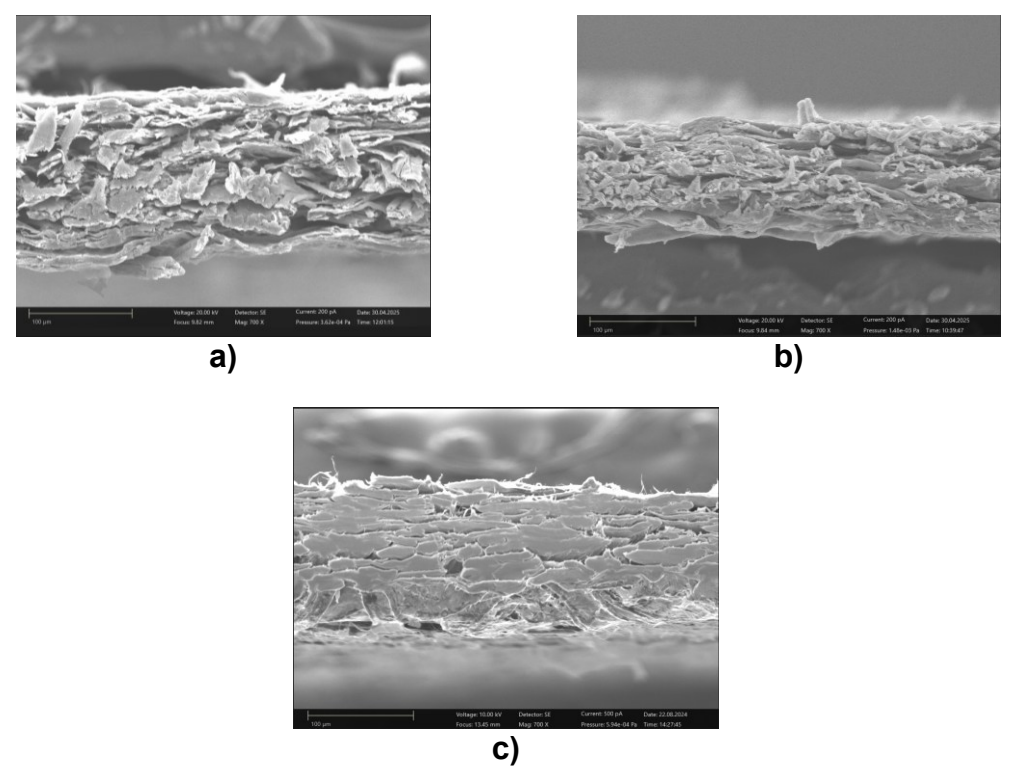


Fig. 11. SEM pictures of 100kWh/t samples. a) 100 kWh/t lab sheet, 700x magnification, b) 100 kWh/t AlCl3/ZnCl2 45Min, 700x magnification, and c) 100 kWh/t NaOH, 700x magnification

Scissors tend to tear or crush fibers and could lead to delamination of layers or the appearance of pores that are bigger than they are. The razor blade can provide a much cleaner, more precise cut that shows a more realistic representation of compaction and bonding. The first set of 100 kWh/t cross-section images can be seen in Fig. 11.

Figure 11a presents the cross section for the untreated 100 kWh/t lab sheet. The cross-section appears to have loosely packed, layered architecture. The fiber layers are irregular and appear to be partially delaminated. There are visible open spaces between layers, which indicate a high porosity and a less compact fiber network. Figure 11b is more compact in structure than a, but still a multi-layered structure can still be observed. There are voids present, but they are less prominent than in a). These observations indicate that an intermediate amount of cellulose regeneration occurred leading to some restructuring and increased packing without a full fusion of fibers. Figure 11c exhibits a cross-section that is more fused and consolidated than the previous two samples. The layers of fibers are still visible, but are more uniformly packed, with fewer voids. The porosity of the material is the lowest among the three samples observed here. This sample likely underwent more effective regeneration treatment, leading to a more cohesive and integrated structure.

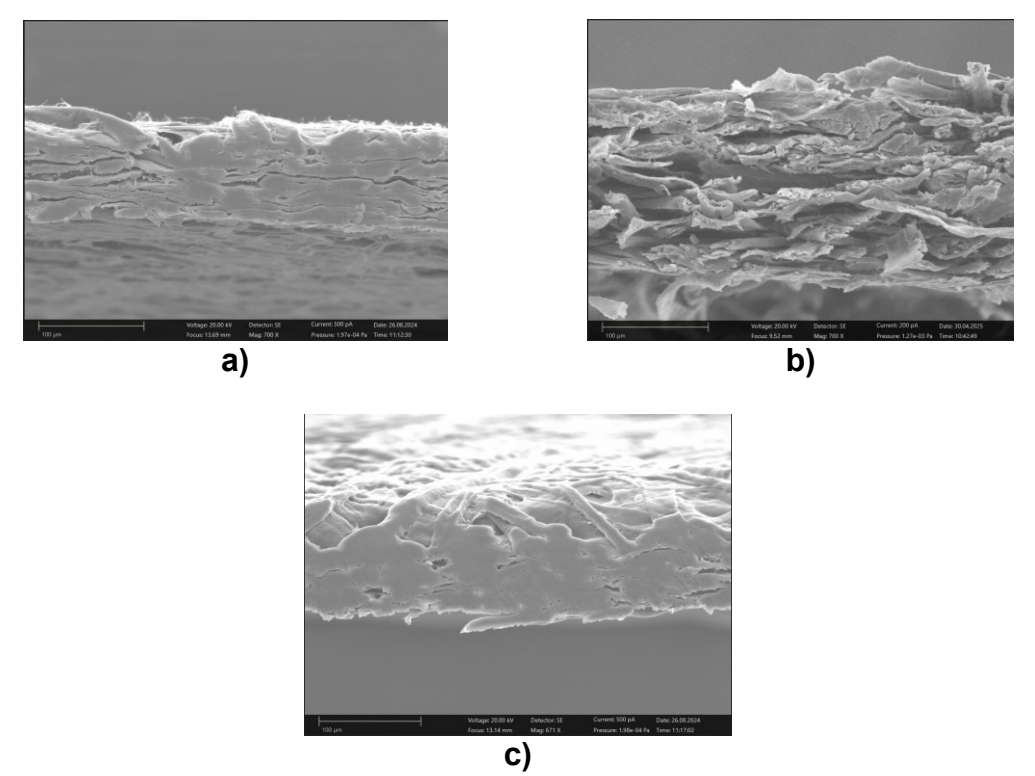


Fig. 12. SEM pictures of 200kWh/t samples. a) 200 kWh/t lab sheet, 700x magnification, b) 200 kWh/t AlCl3/ZnCl2 45Min, 700x magnification, and c) 200 kWh/t NaOH, 700x magnification

In Fig. 12, the cross sections for the 200 kWh/t samples are presented. These samples show the most change in structure due to the use of the razor blade instead of the microscopy scissors. Here, even in Fig. 12a, the untreated paper structure looks very compacted and fused, which cannot reflect the reality of the cross-section of the untreated sample. Figure 12b shows the cross-section of the AlCl₃/ZnCl₂ ACC sample after 45 minutes of treatment. It has a very porous, layered structure, and it looks to be even more porous than the untreated lab sheet in Fig. 11a. Figure 12c displays a mostly fused crosssection with few voids or pores visible. This indicates a very good cellulose II conversion. In this case, it is difficult to determine whether the microscopy scissors had an effect on the sample in Fig. 12b, causing the sample to look more porous than it really was. A phenomenon that is well documented here is that the untreated paper has fibrils that stick out of the material surface in the vertical direction. This is expected for untreated paper samples and is due to the beating of the fibers. On the other hand, in 11c, after the solvent treatment, there were no more fibrils present, and the surface appeared very smooth. This is expected, as the fibrils should be converted by the solvent system first. This phenomenon can be observed again in Fig. 13.

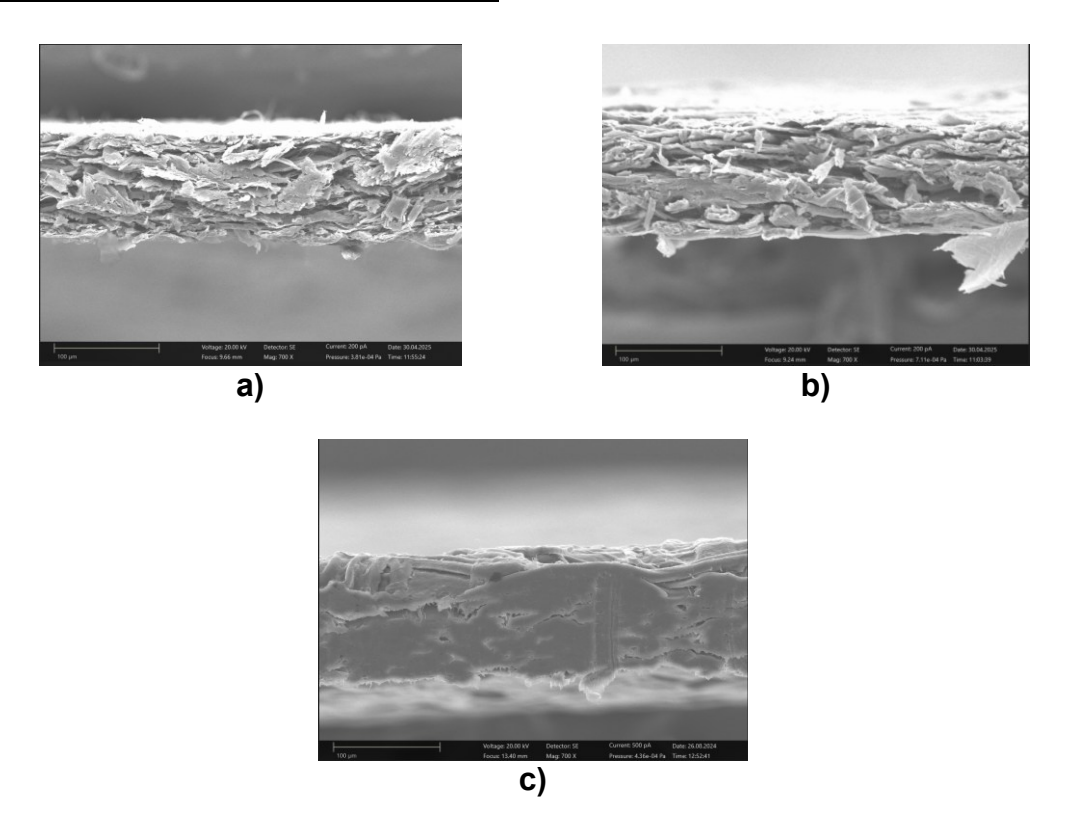


Fig. 13. SEM pictures of 500kWh/t samples. a) 500 kWh/t lab sheet, 700x magnification, b) 500 kWh/t AlCl3/ZnCl2 45Min, 700x magnification, and c) 500 kWh/t NaOH, 700x magnification

Figure 13 displays the 500kWh/t samples both untreated (a) and treated (b, c). Despite 45 minutes treatment of the sample in Fig. 13b, distinct fiber layers were still able to be seen. There appears to be minimal fiber-fiber contact and larger pores than in Fig. 13c. The sample treated with NaOH/urea exhibited in Fig. 13c, has significant bonding between fibers, and low porosity. These observations are indicative of enhanced fiber bonding, which is likely due to the swelling and partial dissolution of fiber surfaces during treatment. The drastic reduction in porosity could be due to the gel-like cellulose redistribution that occurs during regeneration. The compaction of the structure and the formation of a matrix phase when using the NaOH/urea solvent system explains the good mechanical properties and the reduced air permeability. More microscopy experiments must be performed to substantiate the working hypotheses mentioned at the beginning of this article. Due to some differences observed in the cross-section samples *via* SEM, more images should be taken using different preparation methods to ensure that the best images of the ACC materials can be taken without altering the materials' appearance.

Analysis and Need for Further Research

The experiments performed for this work indicate that AlCl₃/ZnCl₂·4H₂O is a promising solvent system for the production of ACCs. The results of the mechanical properties, compared to ACC which was produced with the NaOH/urea solvent system, indicate that there is a need to optimize the process parameters. Research indicates that there is limited dissolution potential for ZnCl₂ salt hydrate systems for cellulose at room temperature. However, upon increasing the temperature of the solvent to 80°C, full dissolution of the cellulose could be achieved (Ma *et al.* 2024). This indicates that increasing the solvent system temperature is favorable to the cellulose dissolution.

Another trial must be done to find a more optimized reaction temperature and the production process must be adjusted accordingly. Cellulose solvent systems using aqueous ZnCl₂ require a specific water content. The water content has been shown to affect the dissolution power of the solvent system. Literature values show that 3.5 parts of water to 1-part ZnCl₂ is the optimal ratio. Potentially another source of improvement can be in adjusting the water-to-salt ratio in the AlCl₃/ZnCl₂·4H₂O solvent system to improve its efficacy (Ma *et al.* 2024). The influence of the solvent system and the raw material pre-treatment on the material properties of ACC as well as the effect on penetration of the solvent system, are interesting research questions that need to be explored in future work. This study has focused primarily on mechanical performance, but future work should include more aspects of biodegradability and environmental impact to further establish the sustainability case for AlCl₃/ZnCl₂-based ACC materials. Experiments concerning the observation of the solvent penetration and the cellulose regeneration are planned, using a confocal microscope. In order to meet the requirements for industrial production, a reduction in the duration of the neutralization process would be of interest.

CONCLUSIONS

- 1. The tests carried out show that the novel solvent system AlCl₃/ZnCl₂·4H₂O is suitable for the production of all-cellulose composites (ACC).
- 2. Compared to ACC manufactured using NaOH/urea, comparable Young's-modulus, and wet strengths were achieved using the AlCl₃/ZnCl₂·4H₂O solvent system. However, the tensile strength and barrier effect against air permeability were worse.
- 3. Changes in the material properties using AlCl₃/ZnCl₂·4H₂O already occur at room temperature, which indicate changes in the microstructure. However, greater improvements in the mechanical properties under tensile load in the dry and wet state are achieved in particular at an increased temperature of 45°C during the dissolution process.
- 4. The wet strength achieved shows that, for certain applications, converting paper into ACC can be an alternative to using conventional wet strength agents.
- 5. An increase in beating energy leads to a reduced wet strength for ACC, when using the NaOH/urea solvent system. By contrast, the barrier effect against air is improved and the tensile strength and the modulus of elasticity are not noticeably affected.

ACKNOWLEDGMENTS

The work was supported within the program for promoting the Industrial Collective Research (IGF) of the Federal Ministry of Economic Affairs and Climate Action (BMWK), based on a resolution of the German Parliament.

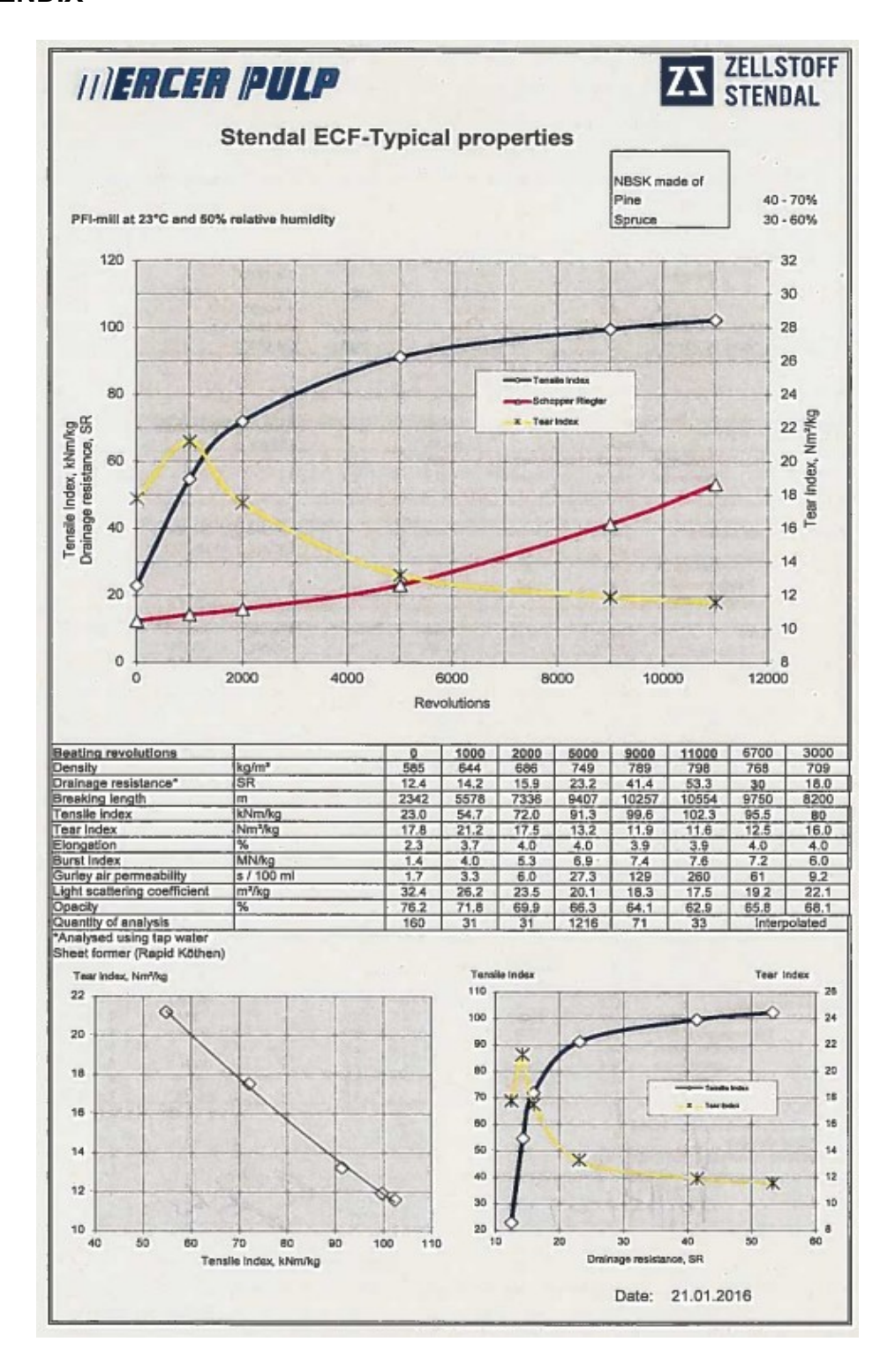
REFERENCES CITED

- Baghaei, B., and Skrifvars, M. (2020). "All-cellulose composites: A review of recent studies on structure, properties and applications," *Molecules* 25(12), article 2836. DOI: 10.3390/molecules25122836
- Bouchard, J., Méthot, M., Fraschini, C., and Beck, S. (2016). "Effect of oligosaccharide deposition on the surface of cellulose nanocrystals as a function of acid hydrolysis temperature," *Cellulose* 23, 3555-3567. DOI: 10.1007/s10570-016-1036-5
- DIN 54514 (2008). "Testing of paper and board Determination of the initial wet web strength by tensile test," Deutsches Institut für Normung e.V., Berlin, Germany.
- Guzman-Puyol, S., Ceseracciu, L., Tedeschi, G., Marras, S., Scarpellini, A., Benitez, J. J., Athanassiou, A., and Heredia-Guerrero J.A. (2019). "Transparent and robust all-cellulose nanocomposite packaging materials prepared in a mixture of trifluoroacetic acid and trifluoroacetic anhydride," *Nanomaterials (Basel)* 9(3), article 368. DOI: 10.3390/nano9030368
- Huber, T., Müssig, J., Curnow, O., Pang, S., Bickerton, S., and Staiger, M. P. (2011). "A critical review of all-cellulose composites," *Journal of Materials Science* 47(3), 1171–1186. DOI: 10.1007/s10853-011-5774-3
- ISO 187 (2022). "Paper, board and pulps Standard atmosphere for conditioning and testing and procedure for monitoring the atmosphere and conditioning of samples," International Organization for Standardization, Geneva, Switzerland.
- ISO 1924-3 (2005). "Paper and board Determination of tensile properties Part 3: Constant rate of elongation method (100 mm/min)," International Organization for Standardization, Geneva, Switzerland.
- ISO 5269-2 (2004). "Pulps Preparation of laboratory sheets for physical testing Part
 2: Rapid-Köthen method," International Organization for Standardization, Geneva,
 Switzerland.
- ISO 5636-5 (2013). "Paper and board Determination of air permeance (medium range). Part 5: Gurley method," International Organization for Standardization, Geneva, Switzerland.
- Jahn, P., Walz, U., Valkama, J.-P., and Schabel, S. (2022). "All-cellulose composite für anspruchsvolle Verpackungsaufgaben," DOI: 10.26083/TUPRINTS-00021502
- Jiao, L., Ma, J., and Dai, H. (2015). "Preparation and characterization of self-reinforced antibacterial and oil-resistant paper using a NaOH/urea/ZnO solution," *PLoS One* 10, article e0140603. DOI: 10.1371/journal.pone.0140603
- Letters, K. (1932). "Viskosimetrische Untersuchungen über die Reaktion von Zellulose mit konzentrierten Chlorzinklösungen," *Kolloid-Zeitschrift* 58, 229–239. DOI: 10.1007/BF01460731
- Lu, X., and Shen, X. (2011). "Solubility of bacteria cellulose in zinc chloride aqueous solutions," *Carbohydrate Polymers* 86(1), 239-244. DOI: 10.1016/j.carbpol.2011.04.042
- Ma, J., Wang, Z., Zhou, X., and Xiao, H. (2015). "Self-reinforced grease-resistant sheets produced by paper treatment with zinc chloride solution," *BioResources* 10(4), 8225-8237. DOI: 10.15376/biores.10.4.8225-8237
- Ma, J., Zhou, X., Xiao, H., and Zhao, Y. (2018). "Effect of NaOH/urea solution on enhancing grease resistance and strength of paper," *Nordic Pulp & Paper Research Journal* 29(2), 246-252. DOI: 10.3183/npprj-2014-29-02-p246-252

- Ma, W., Li, X., Zhang, L., Zheng, Y., Xi, Y., Ma, J., and Wang, Z. (2024). "Novel insights on room temperature-induced cellulose dissolution mechanism *via* ZnCl₂ aqueous solution: Migration, penetration, interaction, and dispersion," *International Journal of Biological Macromolecules* 272, article 132912. DOI: 10.1016/j.ijbiomac.2024.132912
- Shi, C., Zhang, L., Shi, Z., Yan, M., Wang, Z., and Ma, J. (2023). "Complete utilization of AlCl₃/ZnCl₂ aqueous solution to produce lignin-containing cellulose films with controlled properties," *Industrial Crops and Products*, article 116200. DOI: 10.1016/j.indcrop.2022.116200
- Tanaka, A., Khakalo, A., Hauru, L., Korpela, A., and Orelma, H. (2018). "Conversion of paper to film by ionic liquids: Manufacturing process and properties," *Cellulose* 25(10), 6107-6119. DOI: 10.1007/s10570-018-1944-7
- Tervahartiala, T., Hildebrandt, N. C., Piltonen, P., Schabel, S., and Valkama, J. (2018). "Potential of all-cellulose composites in corrugated board applications: Comparison of chemical pulp raw materials," *Packaging Technology and Science* 31(4), 173-183. DOI: 10.1002/pts.2365
- Tian, Y., Zhang, L., Li, X., Yan, M., Wang, Y., Ma, J., and Wang, Z. (2023). "Compressible, anti-freezing, and ionic conductive cellulose/polyacrylic acid composite hydrogel prepared *via* AlCl₃/ZnCl₂ aqueous system as solvent and catalyst," *International Journal of Biological Macromolecules* 253(Pt 1), article 126550. DOI: 10.1016/j.ijbiomac.2023.126550
- Xi, Y., Zhang, L., Tian, Y., Song, J., Ma, J., and Wang, Z. (2022). "Rapid dissolution of cellulose in an AlCl₃/ZnCl₂ aqueous system at room temperature and its versatile adaptability in functional materials," *Green Chemistry* 24(2), 885-897. DOI: 10.1039/d1gc03918k
- Yousefi, H., Nishino, T., Faezipour, M., Ebrahimi, G., and Shakeri, A. (2011). "Direct fabrication of all-cellulose nanocomposite from cellulose microfibers using ionic liquid-based nanowelding," *Biomacromolecules* 12(11), 4080-4085. DOI: 10.1021/bm201147a
- Yousefi, H., Mashkour, M., and Yousefi, R. (2015). "Direct solvent nanowelding of cellulose fibers to make all-cellulose nanocomposite," *Cellulose* 22(2), 1189-1200. DOI: 10.1007/s10570-015-0579-1

Article submitted: January 28, 2025; Peer review completed: April 8, 2025; Revised version received: July 5, 2025; Accepted: July 8, 2025; Published: July 28, 2025. DOI: 10.15376/biores.20.3.7617-7646

APPENDIX



Mercer Pulp Stendal ECF

General Properties	Typical values	Guarantee value	Unit	Method SCAN	Method EN ISO	Frequenc	у
ISO Brightness	89.5	> 88.5	% ISO	-	3688	- 1	Day
Sheet brightness	88.8	1.	%		2470	24	Day
Brightness reversion	3.8		%	-	5630-1*	1	Day
Dirt count	1.0	< 3	mm ⁴ /kg	-	5350-2	48	Day
Dirt count	1.0	< 3	ppm	-	5350-2	48	Day
Intrinsic Viscosity	727	> 600	ml/g		5351	6	Day
Extractives	0.06	< 0.10	%	CM 49 03		4	Month
- Ash	0.18	< 0.30	%		1762	4	Month
pH	5.2	> 5.00		P 14:65**		4	Month
Organic chlorine in pulp	63	< 100	mg/kg	CM 52:94		12	Month
AOX removable by washing	3	< 5	mg/kg	CM 44:97		4	Month

bre dimensions, Pulp Eye	Typical values	Unit	Range ±2 SD***	CoV****	Method SCAN	Method EN ISO	Frequency
Fibre lengti	2.10	mm	0.09	2.1			Continous
Fibre widtl	28.2	um	0.7	1.2	-		Continous

Preparation of test samples	Target	Variation	Unit	Method SCAN	Method EN ISO	
Temperature	23	±1	*C		187	Continous
Relative humidity Preparation of laboratory sheets	50	±2	% RH		187 5269-2	Continous

Physical Properties	Typical value	Unit	Range ± 2 SD***	CoV****	Method SCAN	Method EN ISO	Fn	equency
PFI beating revolutions	0					5264-2	100	
Water Retention Value	1.10	g H2O/g pulp	0.06	2.5	C 62:00		1	Day
Density	585	kg/m*	640	54.7	-	534	1	Day
Drainage resistance	12	SR	5	18.5		5267-1	1	Day
Breaking length	2342	m	201	4.3			1	Day
Tensile index	23.0	kNm/kg	2.0	4.3		1924-3	1	Day
Tear index	17.8	Nm³/kg	10.7	30.1		1974	1	Day
Burst index	1.4	MN/kg	0.2	6.1	-	2758	1	Day
PFI beating revolutions	2000					5264-2		
Density	686	kg/m³	15	1.1		534	4	Month
Drainage resistance	16	SR	1	3.7		5267-1	4	Month
Breaking length	7336	m	398	2.7			4	Month
Tensile index	72.0	kNm/kg	3.9	2.7		1924-3	4	Month
Tear index	17.5	Nm³/kg	1.6	4.5		1974	4	Month
Burst Index	5.3	MN/kg	0.4	3.3	-	2758	4	Month
PFI beating revolutions	5000			100000		5264-2		history
Density	749	kg/m*	20	1.3		534	6	Day
Drainage resistance	23	SR	2	4.4		5267-1	6	Day
Breaking length	9407	m	472	2.5	-		6	Day
Tensile index	91.3	kNm/kg	4.6	2.5		1924-3	6	Day
Tear Index	13.2	Nm*/kg	1.9	7.2		1974	6	Day
Burst index	6.9	MN/kg	0.5	3.5		2758	6	Day
PFI beating revolutions	9000			40.0	-	5264-2		
Density	789	kg/m³	32	2.0	-	534	8	Month
Drainage resistance	41	SR	8	9.5		5267-1	8	Month
Breaking length	10257	m	578	2.8			8	Month
Tensile index	99.6	kNm/kg	5.7	2.8		1924-3	В	Month
Tear index	11.9	Nm³/kg	1.1	4.4		1974	8	Month
Burst Index	7,4	MN/kg	0.5	3.6		2758	8	Month

* time 24 h
** use of KCI instead of delon. Water

*** standard deviation !
**** coefficient of variation SD*100/a

Koppensteiner Managing Director

i, V. Dr. Martin Zenker Manager Technology & Customer Support

Date: 21.01.2016

Estimated Material Porosity using Image J for Figure 8 images a) – f)

Image J Analysis of 100 kWh/t Samples from Figure 8

Figure 8 Image	Estimated Porosity (%)
a)	43.470
b)	42.983
c)	43.481
d)	40.621

